Chinese Journal of
POLYMER SCIENCE

RESEARCH ARTICLE

https://doi.org/10.1007/s10118-026-3711-9
Chinese J. Polym. Sci.

Sliding Dynamics of Ring Chain on a Rod-Coil Block Copolymer in Rotaxane

Si-Yi Yan[a], Xiang-Hong Wang[b*], Ke Li[c*], and Lin-Li He[a*]

[a] *Department of Physics, Wenzhou University, Wenzhou 325035, China*
[b] *Shanghai Technical Institute of Electronics & Information, Shanghai 201411, China*
[c] *College of Electronics and Information Engineering, Shanghai University of Electric Power, Shanghai 200090, China*

Abstract Rotaxanes are a class of mechanically interlocked polymers characterized by the sliding motion of ring molecules along a linear backbone. The dynamic behavior of a ring plays a critical role in determining its material properties. In this study, molecular dynamics simulations were performed to investigate the sliding dynamics of a ring on a rod-coil copolymer in rotaxane. We find that both the mean square displacement $g_3(t)$ and the diffusion coefficient D of the rings are influenced by the rod-to-coil length ratio α, the stretching degree μ of the coil block, and the ring size N_{ring}. The mean square displacement $g_3(t)$ shows sub-diffusive behavior at intermediate time scales owing to the heterogeneous backbone. The diffusion coefficient exhibits nonmonotonic dependence on α and μ. D first decreased and then increased as α increased, indicating that the ring diffused faster on more homogeneous copolymer chains. D increases with μ under a moderate stretching degree of the coil block, but decreases under near full extension, which demonstrates that the dynamics of the ring are governed by a competition between the chain flattening and the coil block's fluctuation. Similarly, ring size N_{ring} has a nonmonotonic influence on the diffusion coefficient D. This study provides molecular-level insights into the manipulation of sliding dynamics in rod-coil-based rotaxanes, thereby offering a theoretical basis for the design of functional slide-ring materials through topological control.

Keywords Molecular dynamics simulation; Sliding dynamics; Rod-coil copolymer

Citation: Yan, S. Y.; Wang, X. H.; Li, K.; He, L. L. Sliding dynamics of ring chain on a rod-coil block copolymer in rotaxane. *Chinese J. Polym. Sci.* https://doi.org/10.1007/s10118-026-3711-9

INTRODUCTION

Rotaxanes, initially reported by Harrison *et al.*,[1] are a class of mechanically interlocked molecules in which one or more macrocycles are encircled by linear molecular axles bearing bulky stoppers at both ends.[2–7] Polyrotaxanes (PR) are polymers that incorporate repeating rotaxane motifs in their structures.[8] Many polyrotaxanes have been synthesized and applied as polymeric materials.[9–12] Harada *et al.* successfully synthesized polyrotaxanes through spontaneous self-assembly driven by host-guest interactions between α-cyclodextrin and polyethylene glycol chains in an aqueous solution.[13] Okumura and Ito fabricated a slide-ring gel based on polyrotaxanes with slidable figure-of-eight cross-links.[14] Furthermore, PR has been applied in molecular machines.[15–18] For example, in a molecular shuttle, the position of the ring on the backbone is regulated by external stimuli such as temperature,[19] pH,[20] or light.[21]

A distinctive feature of rotaxanes is that the macrocyclic components can slide along the axial polymer chain owing to the topological confinement. This dynamic behavior originates from the advantageous nature of the mechanical bond, specifically, the low energy barrier for the rotation of the rings or their translation along the polymeric thread.[8] The position and mobility of these macrocycles are crucial determinants of the functionality and properties.[22,23] Therefore, exploring the sliding dynamics of the rings in rotaxanes plays a key role in understanding the rotaxane system and has attracted considerable attention.[24–26] Yasuda *et al.* investigated the relative motion between rings and polymer chains using molecular dynamics simulations.[27] They found that the rings exhibited faster sliding diffusion along the fluctuating chain than along the fixed chain. Mayumi *et al.* probed the conformational evolution of polyrotaxane as a function of concentration *via* small-angle neutron scattering. Their results indicate that while cyclic molecules slide freely along the polymer axis in dilute regimes, the mobility of the ring is substantially suppressed upon concentration increase owing to enhanced inter-ring interactions.[28]

Growing interest has focused on polyrotaxanes based on rod-coil block copolymer backbones.[29–31] By harnessing the combined properties of orientable rigid rods and adaptable flexible coils,[32] this unique architecture enables the creation of supramolecular materials with hierarchical organization and dynamic functionality. Using Brownian dynamics simulations coupled with length-dependent kinetic theory, Gao *et al.* systematically investigated the living supramolecular poly-

* Corresponding authors, E-mail: wangxianghong@stiei.edu.cn (X.H.W.)
E-mail: ke.li@shiep.edu.cn (K.L.)
E-mail: linlihe@wzu.edu.cn (L.L.H.)
Received February 21, 2026; Accepted April 9, 2026; Published online July 6, 2026

merization of rigid cylindrical micelles by employing the seeded growth of rod-coil block copolymers as a model system. Their study revealed that the micelle length governs a marked transition in growth kinetics, which is attributed to the rigidity and restricted diffusion behavior of the micelles, which is driven by the epitaxial propagation of a liquid crystalline structure and represents a diffusion-controlled process.[33] The rod-coil block copolymer backbones in polyrotaxanes enable entropy-driven localization of rings and tunable sliding dynamics, allowing precise control over ring distribution and mobility, which in turn enhances the mechanical properties and dynamic functionality of the material.[34–39] Ito *et al.* employed a poly(ethylene oxide)-*b*-poly(propylene oxide)-*b*-poly-(ethylene oxide)(PEO-PPO-PEO) triblock copolymer as the backbone to control *β*-cyclodextrins (*β*-CD) on the PPO chain[35] and revealed that the macroscopic mechanical properties of the system can be effectively tuned by altering the position of the rings along the polyrotaxane backbone. We can also control the location of the rings on the polyrotaxane by tuning the interactions between the rings and backbone, for instance, through the introduction of coordination or covalent bonds.[40–42]

Molecular dynamics simulation is a computational method that computes and tracks the trajectory of each atom in a system over time using Newton's equations of motion at the atomic scale, thereby uncovering the microscopic structures and dynamic processes.[43,44] To simulate polymer dynamics, Kremer and Grest developed a coarse-grained bead-spring model[45] which has been widely adopted for the analysis and visualization of molecular motion in polymer systems. Because of the critical role of ring positioning and sliding dynamics along the polymer backbone in determining the physical properties of PR and its derivatives, Wang *et al.* proposed an entropy-based method to control both ring positioning and sliding dynamics along the PR in the modeling of rod-coil-rod triblock copolymers.[34] The results show that the rings prefer to reside in the rod block regions because of entropy reduction in the coil blocks. However, the relative motion between the rings and the backbone of the rod-coil block copolymer was not discussed.

In this study, we investigated the sliding dynamics of a ring on a rod-coil block copolymer in rotaxane using molecular dynamics simulations. A coarse-grained model is presented as a rotaxane with a ring threaded on a rod-coil block copolymer with a rod block length of N_r and a coil block length of N_f. We focus on the influence of the rod-to-coil length ratio α and the stretching degree of the coil block μ on the diffusion motion of the rings while simultaneously considering the effects of the ring size N_{ring}.

MODEL AND METHOD

The coarse-grained model for the rotaxane system consisted of a rigid ring threaded onto an axial block copolymer backbone. The backbone comprises a rod (blue line) of N_r monomers and a coil (red line) strand of N_f monomers, as shown in Fig. 1. In this study, the coil block length N_f was fixed at $N_f = 60$. The ring is modeled as a ring polygon, and the ring size can be modified by varying the number of monomers N_{ring}. The model system can be characterized by three parameters: the ratio of the rod to coil length $\alpha = \frac{N_r}{N_f}$, relative extension of the coil strand $\mu = \frac{R_{ee}}{R_{max}}$, and ring size N_{ring}. Here, R_{ee} denotes the root mean square end-to-end distance of the coil chain and $R_{max} = N_f \times b$ is its contour length, with b representing the bond length. All monomers had the same mass m and diameter σ.

The truncated and shifted Lennard-Jones (LJ) potential, known as the Week-Chandler-Andersen (WCA) potential,[46] can be employed to describe the interactions between any two non-bonded monomers,[47,48]

$$U_{LJ}(r) = \begin{cases} 4\varepsilon\left[\left(\frac{\sigma}{r}\right)^{12} - \left(\frac{\sigma}{r}\right)^{6} + \frac{1}{4}\right], r \le r_C \\ 0, r > r_C \end{cases} \quad (1)$$

where ε is the depth of the potential well, representing the characteristic unit of energy, and σ is the unit of the length. r is the distance between one pair of monomers, and the cutoff distance r_C was set as $2^{1/6}\sigma$.

The bonded interactions between all neighboring monomers within the polymer backbone and rings are represented by the FENE-LJ potential.[45]

$$U_{bond}(r) = U_{FENE}(r) + U_{LJ}(r) \quad (2)$$

where

$$U_{FENE} = -\frac{KR_0^2}{2}\ln\left[1 - \left(\frac{r}{R_0}\right)^2\right], r < R_0 \quad (3)$$

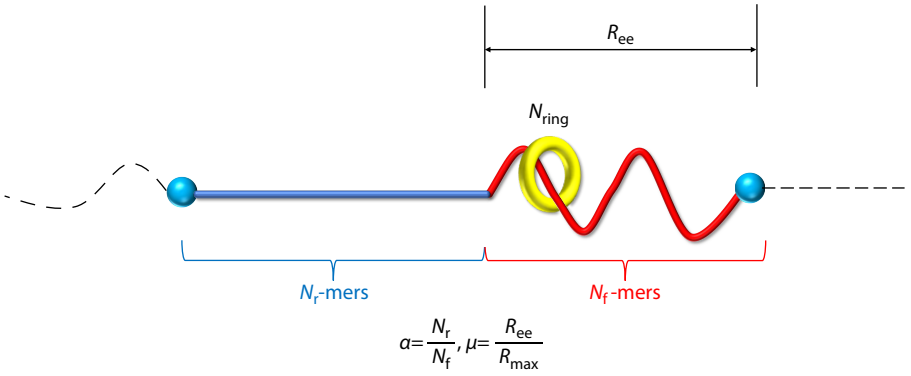

Fig. 1 Schematic illustration of rotaxane consisting of a rod-coil copolymer threaded by a ring chain, where N_r and N_f are the numbers of monomers in rod and coil blocks, respectively, and R_{max} denotes the contour length of the coil chain, *i.e.*, $R_{max} = N_f \times b$ with b representing the bond length.

https://doi.org/10.1007/s10118-026-3711-9

Here, the spring constant K was set to $K = 30k_BT/\sigma^2$, and the maximum extension of the spring was $R_0 = 1.5\sigma$.

The rigidity of the chain is modeled by the angle-bending potential applied to each set of three consecutive beads:[27,49,50]

$$U_{\text{bending}} = \frac{1}{2}k_b[\theta - \theta_0]^2 \quad (4)$$

where the bending constant k_b represents the bending energy, and θ denotes the angle between two consecutive bonds. To ensure a flexible rod-coil copolymer and rigid ring, the bending energy k_b was chosen as $k_b = 0$ for the axial block copolymer and $k_b = 100k_BT/\text{rad}^2$ for the ring. θ_0 is the internal angle of an N-sided regular polygon. Here, $\theta_0(N_{\text{ring}}) = 180[(N_{\text{ring}} - 2)/N_{\text{ring}}]$ for the ring chain with N_{ring} monomers.

The constant temperature of the system is controlled by the Langevin thermostat, and the motion of all monomers is described by[51,52]

$$m\frac{d^2r_i}{dt^2} = F_i(t) - m\gamma\frac{dr_i}{dt} + F_i^R \quad (5)$$

where m represents the mass of the monomer, r_i is the position of the i-th monomer, and $F_i(t)$ is the conservative force resulting from the addition of the Lennard-Jones, FENE, and angle-bending terms. The friction constant γ was set to $\gamma = 0.5\tau^{-1}$. $F_i^R(t)$ is the noise force and satisfies the fluctuation-dissipation theorem:

$$\left\langle F_i^R(t)F_j^R(t')\right\rangle = 2k_BT\gamma\delta_{ij}\delta(t-t') \quad (6)$$

Here, the temperature T was fixed at $T = 1$ in units of ε/k_B, where k_B is the Boltzmann constant. The time step was $\tau_0 = 0.01\tau$. In this work, all the measurements were performed in LJ units, where the units of energy, length, mass, and time were taken to be 1 (*i.e.*, $\varepsilon = \sigma = m = 1$, $\tau = (m\sigma^2/\varepsilon)^{\frac{1}{2}} = 1$).

All molecular dynamics simulations were performed using the Large-scale Atomic/Molecular Massively Parallel Simulator (LAMMPS) package.[53] In our simulations, a single ring was threaded onto a rod-coil block copolymer chain and embedded within a simulation box with dimensions of $100 \times 100 \times L_Z$. In the initial configuration, the ring was randomly positioned along the backbone, and each independent simulation run used a different random seed to generate its initial position, thereby ensuring that all simulations started from random configurations. This guarantees that the reported diffusion results represent the equilibrium dynamics of the system and are not biased by the initial ring location. The rod-coil block copolymer chain ends were connected under periodic conditions to prevent the ring from dethreading, which realizes a periodically connected chain. L_Z is defined as the end-to-end distance of the rod-coil copolymer. Because the rod block is a fixed rod-like chain, the bond length of the rod block chain remains at 1σ, and the position of the monomer for the rod block is fixed during the simulation process. Thus, L_Z is the sum of the end-to-end distance of the rod block and coil block, that is, $L_Z = N_r + R_{ee}$. The rod-coil copolymer was aligned along the z-axis, and we confirmed that the rings were not detached from the axial copolymer.

To evaluate the sliding dynamics of the ring along the rod-coil polymer in the rotaxane, we calculated the mean square displacement (MSD), $g_3(t)$, of the center of mass of the ring in coordinates along the backbone of the rod-coil polymer. Here, $g_3(t)$ is described by:[27,54]

$$g_3(t) = b^2 < [i(t) - i(0)]^2 > \quad (7)$$

where the bond length of the rod-coil polymer was $b = 1\sigma$. $i(t)$ denotes the index number of the monomer in the backbone of the rod-coil polymer closest to the ring, which is sequentially assigned to the monomers of the backbone from one end to the other with the period considered. The brackets <> represent the statistical average. Based on $g_3(t)$, the diffusion coefficient of the ring along the rod-coil polymer is estimated as

$$D = \lim_{t\to\infty}\frac{g_3(t)}{2t} \quad (8)$$

Here, $g_3(t)$ was calculated in the time range of $0 < t < 10^8$. To reduce the size of the output data, simulations were performed with different time ranges ($10 < t < 10^2$, $10^2 < t < 10^3$, $10^3 < t < 10^4$, and $10^4 < t < 10^6$), and $g_3(t)$ was calculated for $10 < t < 100$, $100 < t < 10^3$, $10^3 < t < 10^4$, and $10^4 < t < 10^6$. The data output intervals were 10, 100, 1000, and 10000 for the corresponding time ranges. For statistical accuracy, we conducted 500 simulation runs for each time range, and all the data for $g_3(t)$ were obtained by averaging these simulation runs.

RESULTS AND DISCUSSION

Effects of the Rod-to-coil Ratio α

In this section, the influence of the rod-to-coil ratio, α, on the sliding dynamics of the ring is investigated. We focused on the diffusion motion of the ring along the rod-coil copolymer of various α. Here, the relative extension of the coil block was fixed at $\mu = 0.23$, which corresponds to that of the coil strand in the dilute solution. The length ratio between the rod and coil blocks, α, was varied from zero to seven by adjusting the rod block length, N_r. Fig. 2 illustrates the time evolution of $g_3(t)$ for a ring with a ring size of N_{ring}=10 (a) and N_{ring}=12 (b) for various α. As shown in Fig. 2(a), for the case of $\alpha = 0.03$ and $\alpha = 0.07$, $g_3(t)$ exhibits a linear time dependence, where N_r is so small that the rod-coil copolymer backbone can be approximated as a flexible chain. In other cases, the $g_3(t)$ curve displays three distinct regimes. In the short-time regime ($0<t<10^3$), the curves nearly overlap, $g_3(t) \sim t^\beta$ and $\beta \approx 1$, indicating that the ring moves freely within the homogeneous rod block or coil block. In the long-time regime, the ring motion exhibits long-time normal diffusion, characterized by $g_3(t) \sim t$. In the intermediate time regime, a clear subdiffusive behavior was observed. To elucidate the intermediate-time sub-diffusion in detail, we fitted the data using a power-law relationship $g_3(t) \sim t^\beta$ and extracted the scaling exponent β and the fitting range. The original data and fitted curves for the ring's subdiffusive regime are shown in the inset of Fig. 2(a). As observed in the inset of Fig. 2(a), $\beta = 0.83$ with $2\times10^3 < t < 2\times10^4$ for $\alpha = 1$, $\beta = 0.86$ with $9\times10^3 < t < 5\times10^4$ for $\alpha = 2.5$, and $\beta = 0.88$ with $10^4 < t < 9\times10^4$ for $\alpha = 3.3$, confirming the sub-diffusive behavior in the intermediate time regime. This phenomenon can be attributed to the heterogeneous architecture of the rod-coil copolymer backbone, and the ring prefers to locate on the rod blocks, which has also been reported in literature.[34] In the diffusion process, when the ring slides the distance of the rod-block length, it encounters the rod-coil interface, and the probability of the ring passing

through this interface vanishes, resulting in slower dynamics and the onset of the sub-diffusive regime. Thus, we find that the subdiffusive regime starts at a later time for $\alpha = 2.5$ compared with that of $\alpha = 1$ in Fig. 2(a). After the Brownian motion shuttling action, the ring can slide through the rod-coil interface. Consequently, the sub-diffusive regime ends, followed by a long-time normal diffusive regime. Moreover, a similar α dependence of $g_3(t)$ for N_{ring}=12 is also observed in Fig. 2(b), and the subtle intermediate-time sub-diffusion suggests that larger rings can more readily traverse the rod-coil interface.

The sliding dynamics of the rings along the rod-coil copolymer backbone can be characterized by the diffusion coefficient of the ring, D. As shown in Fig. 3(a), the diffusion coefficient D exhibits a similar nonmonotonic dependence on α for the three different ring sizes. The diffusion coefficient, D, first decreases and then increases with an increase in α. This behavior can be interpreted from the perspective of the energy gap ΔE of the system within the framework of the transition state theory.[34] The theory states that once the energy barrier exceeds the thermal energy (*i.e.*, $\Delta E > k_B T$), transitions between the involved states become increasingly rare, and the transition time increases exponentially with the barrier height. The current system is a typical two-state system, where the ring remains on either the rod block or the coil block. Because the two states have different energy levels, there is an energy barrier when the ring slides on the rod-coil copolymer. At a small α, the rod segments are short, and the backbone resembles a flexible chain with strong thermal fluctuations and a relatively low energy barrier, thereby facilitating ring sliding and yielding the highest observed D values. As α increaseds, the increasing rod-block length enhanceds the heterogeneity of the backbone and raiseds the sliding barrier, making the diffusion of the ring more difficult and leading to a decrease in D. When α exceeds a certain threshold, the heterogeneity of the backbone decreases, and the backbone structure gradually homogenizes into a rod-like chain, which leads to an increase in the diffusion coefficient D. To further explain the non-monotonic behavior of D with respect to α, we calculated the potential of mean force (PMF), $V(x)$, of the ring threaded on the rod-coil copolymer, which is given as:[55]

$$V(x) = -k_B T \ln P(x) \tag{9}$$

where $P(x)$ denotes the probability of the ring being located at the x-th segment of the backbone. The PMFs were considered within one period, where x varied from $x = 1$ (corresponding to the ring closest to the first monomer in the rod block) to $x = N_r + N_f$ (corresponding to the ring closest to the last monomer in the coil block). Fig. 3(b) shows the PMFs of the ring threaded on the rod-coil copolymer for different α with

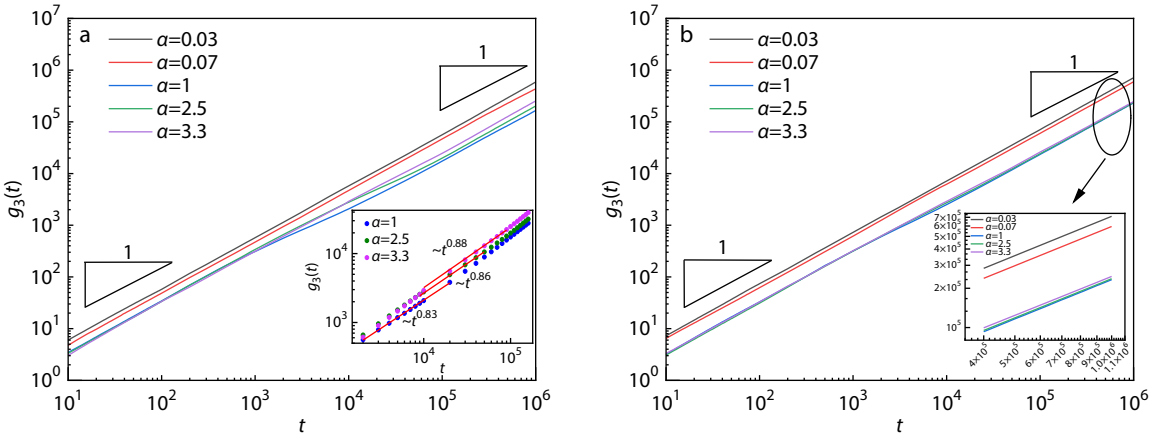

Fig. 2 Time dependence of $g_3(t)$ of the ring threaded on the rod-coil block copolymer with different rod-coil length ratios α. (a) N_{ring}=10; the inset shows a power-law fit $g_3(t) \sim t^{\beta}$ in the intermediate-time window. (b) N_{ring}=12. Here, the stretching degree of the coil block is μ= 0.23.

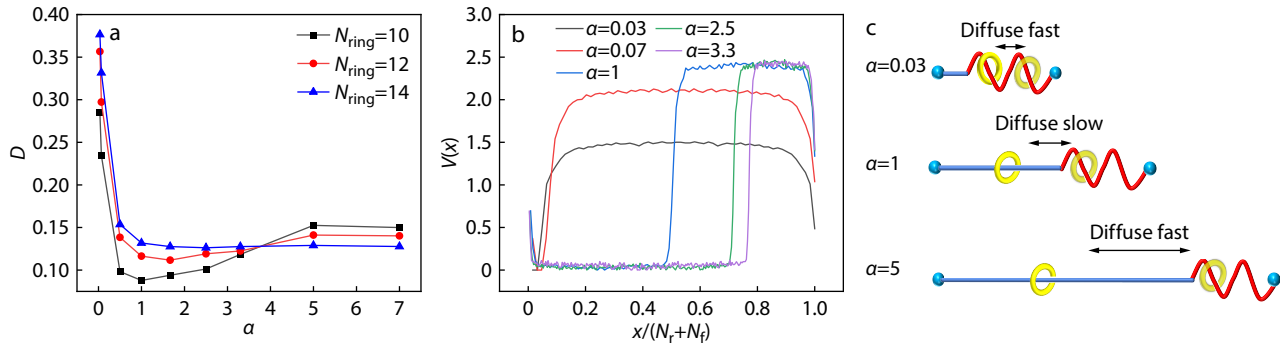

Fig. 3 (a) Diffusion coefficient D of the ring on the rod-coil polymer as a function of the rod-coil length ratio α for different ring sizes N_{ring}; (b) Potential of mean force, $V(x)$, of the ring threaded on the rod-coil block copolymer for different rod-coil length ratios α with N_{ring} = 12; (c) The sliding behavior of a ring under different rod-to-coil length ratios α. Here, the stretching degree of the coil block is μ=0.23.

https://doi.org/10.1007/s10118-026-3711-9

N_{ring} = 12 and μ = 0.23. We found that the PMF shape relies on the rod-to-coil ratio α, and there exists a free energy barrier for the ring to diffuse from the rod block to the coil block. According to Fig. 3(b), the free energy potential barrier ΔE increases with an increase in α for $\alpha \leq 1$, which leads to a decrease in the diffusion coefficient D. With a further increase α, the height of the energy barrier remains nearly constant, but the width of the energy barrier decreases. Because the wider the energy barrier, the more difficult it is for the ring to jump over the energy barrier, we find that D increases as α increases from α = 1 to 2.5 and 3.3, see Fig. 3(b). These results indicate that the sliding dynamics of the ring on the rod-coil block copolymer are very sensitive to the shape of the free energy potential. As illustrated in Fig. 3(c), the ring exhibits fast diffusion at α = 0.03 and 5 but slow diffusion at α = 1, due to the combined effects of barrier height and width. In addition, the minimum value of D occurred at α = 1 for N_{ring} = 10 and moved to α = 2.5 for N_{ring} = 14. A shift in the minimum position occurs because larger rings are less sensitive to the spatial inhomogeneity of the backbone rigidity. The overall rigidity of the backbone becomes more uniform only when the rod block is sufficiently long (*i.e.*, α is large). Meanwhile, when the ring size was increased from N_{ring} = 10 to 12 and 14, D increased for $\alpha \leq 3.3$, but D decreased for $\alpha \geq 5$, as shown in Fig. 3(a). In the former case, the friction between the ring and the axial copolymer is weakened, and the contribution of the coil-block chain fluctuation increases with increasing ring size; thus, the diffusion coefficient D increases with an increase in N_{ring}. According to Yasuda *et al.*, chain fluctuation can enhance the diffusion of the ring, and the sliding diffusion coefficient increases as the ring size increases for rings threaded onto a fluctuating coil polymer.[27] Our results are in good agreement with their work. For the latter case, rings exhibit one-dimensional diffusion on rod-like polymer as $N_r \gg N_f$, and the sliding dynamics is mainly dominated by the self-diffusion of the ring, in which larger ring diffuses slower.[27]

Effects of the Relative Extension of the Coil Block μ

Next, we investigate the sliding dynamics of rings on polymer backbones with varying relative extensions of the coil block μ. In this section, the ratio of the rod to the coil length is fixed at α = 1 in this section. The relative extension of the coil block in rod-coil polymers, μ, can be modulated by adjusting the end-to-end distance of the coil block R_{ee}. Fig. 4 presents the time evolution of $g_3(t)$ for rings sliding along rod-coil copolymer chains with different μ for ring sizes of N_{ring}=10 (a) and N_{ring}=12 (b). As shown in Fig. 4 (a), for the case of μ = 0.8 and μ = 0.9, $g_3(t)$ varies linearly with time. This indicates that the flexible coil blocks weare nearly fully extended, resembling rigid axial chains, where the ring showeds normal diffusion when sliding along a homogeneous rod-like polymer chain. For the other cases, the observed trends of $g_3(t)$ are consistent with those shown in Fig. 2. In the short-time regime, the curves of $g_3(t)$ almost overlap, and the motion of the ring is normal-diffusive, with $g_3(t) \sim t^{\beta}$ and $\beta \approx 1$. In the long-time regime, the rings exhibit a long-time normal diffusion along the backbone. In the intermediate time regime, a sub-diffusion behavior is observed. Owing to the inhomogeneity of the rod-coil copolymer, there is an energy difference between the ring on the rod block and the ring on the coil block. Ring experiences an energy barrier when diffusing along the rod-coil copolymer, which greatly hinders the diffusion of the ring and leads to sub-diffusion behavior. As the stretching parameter increases from μ = 0.1 to μ = 0.4, the coil block becomes more stretched and oriented. Ring can easily pass through the rod-coil interface; thus, a less obvious sub-diffusive behavior for a larger μ is shown in Fig. 4. In addition, $g_3(t)$ exhibits a similar dependence on μ for N_{ring}=12, as shown in Fig. 4(b). However, a subtle intermediate-time sub-diffusion for a larger ring indicates that a larger ring size reduces frictional interactions between the ring and backbone.

We calculated the sliding diffusion coefficient, D, of the rings along a rod-coil block copolymer with varying degrees of stretching of the coil block μ, as shown in Fig. 5(a). The diffusion coefficient D exhibits a non-monotonic dependence on μ for the three different ring sizes. By increasing the relative extension of the coil block, D first increases and then decreases. This behavior stems from the change in the free energy difference ΔE, for the ring residing in the rigid block versus the coil block with various μ. To quantify the effect of μ on the local orientation fluctuations of the coil block, we calculated the bond vector autocorrelation function $C(t)$, which is defined as

$$C(t) = \left\langle \frac{\boldsymbol{B}(t) \cdot \boldsymbol{B}(0)}{|\boldsymbol{B}(t)|\,|\boldsymbol{B}(0)|} \right\rangle \tag{10}$$

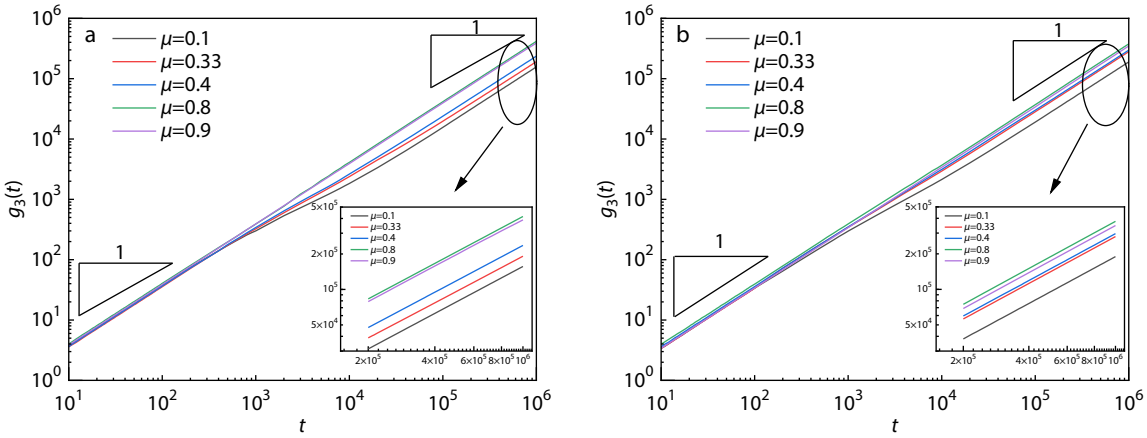

Fig. 4 The time dependence of $g_3(t)$ for the ring threaded on the rod-coil block copolymer with different coil stretching degrees μ for (a) N_{ring} = 10 and (b) N_{ring} = 12. Here, the rod-coil length ratio is α = 1.

https://doi.org/10.1007/s10118-026-3711-9

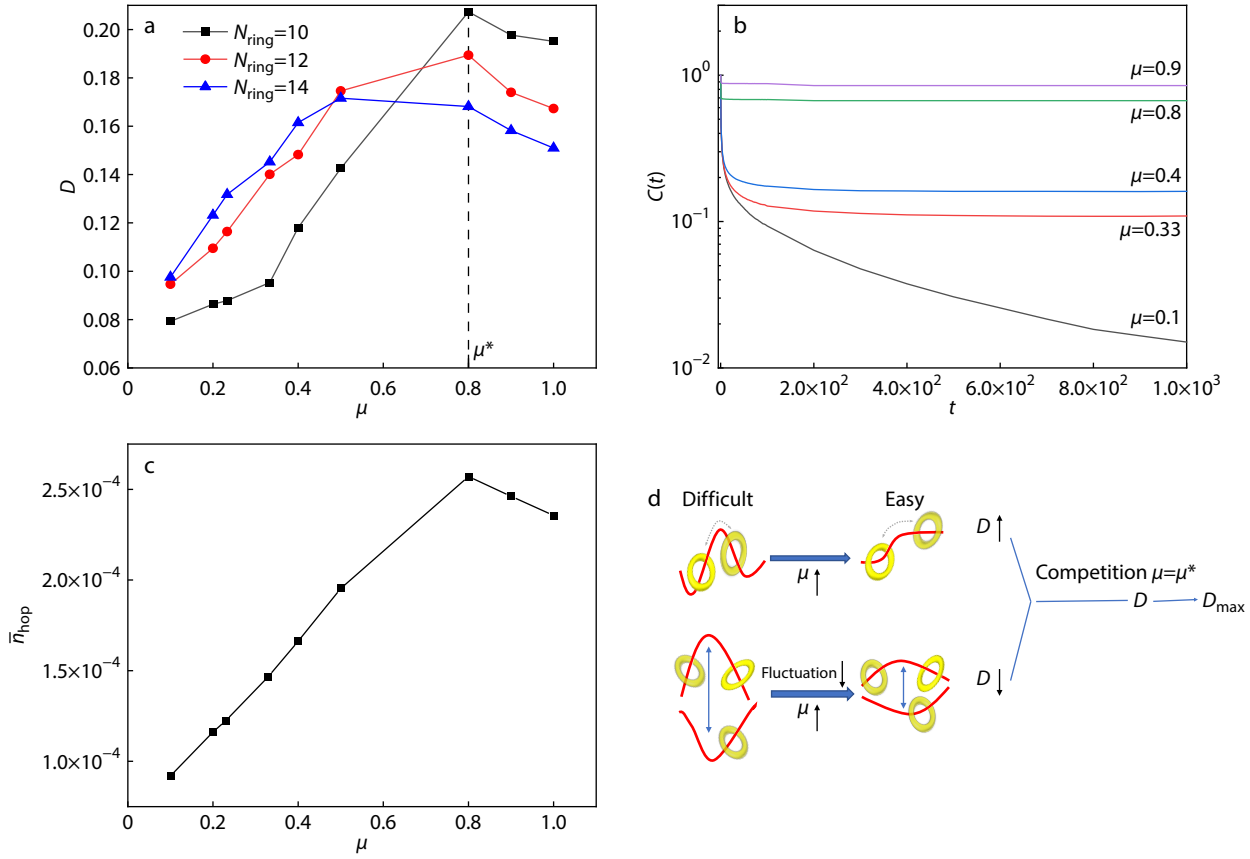

Fig. 5 (a) Diffusion coefficient D of the ring versus the coil stretching degree μ for different ring sizes N_{ring}. μ^* is the critical point. (b) Bond vector autocorrelation function $C(t)$ of the coil chain for different μ with $\alpha = 1$ and $N_{ring} = 12$. (c) Dependence of the average number of hopping events per unit time of the ring, $\bar{n}_{hop}$, on the parameter μ in the rotaxane system with $\alpha = 1$ and $N_{ring} = 12$. (d) The dependence of the ring diffusion on the degree of stretching arises from the competition between the chain flattening and the coil block's fluctuation. Here, the rod-coil length ratio is $\alpha = 1$.

where $\boldsymbol{B}(t)$ is the bond vector at time t, and the average is obtained over all the bonds of the coil chain and over many successive configurations. Fig. 5(b) shows the decay of $C(t)$ for different μ values with $\alpha = 1$ and $N_{ring} = 12$. Increasing μ shifts the $C(t)$ curves to the right, indicating that function $C(t)$ requires more time to decorrelate. For example, at $\mu = 0.1$, the autocorrelation decayeds rapidly, reflecting strong chain fluctuations, whereas at $\mu = 0.9$, the autocorrelation remaineds high over the entire time range, indicating suppressed fluctuations. These results indicate that conformational fluctuations of the coil chain are gradually suppressed as μ increases. At a moderate stretching degree ($0 < \mu < 0.5$), the coil chain is compressed or slightly stretched, and the free energy difference ΔE remains large, which hinders ring diffusion. As μ increaseds, the gradual stretching of the coil block promoteds the diffusion of the ring, and ΔE gradually decreaseds, which ledleads to an increase in D. At a large stretching degree ($\mu > 0.5$), the coil block is significantly stretched, and chain conformational fluctuations are reduced. According to a previous study,[27] chain fluctuations can enhance the sliding motion of the ring along the coil. Thus, the diffusion coefficient of ring D decreases with increasing μ because the fluctuation of the coil block is suppressed.

For the current rod-coil polyrotaxane system, the ring resides on either the rod block or the coil block at any given time, forming a typical two-state system. Fig. 3(b) shows the two distinct states for the ring location, which have different energy levels, confirming the two-state nature. According to transition state theory, when the energy barrier exceeds the thermal energy, transitions between the two states become rare. Consequently, hopping events of the ring from the rod to the coil block occur when $\frac{\Delta E}{k_B T} > 1$. The hopping frequency, $\bar{n}_{hop}$, defined as the average number of hopping events per unit time, was calculated. For a ring threaded on a rod-coil copolymer with $\alpha = 1$ and $N_{ring} = 12$, Fig. 5(c) shows that $\bar{n}_{hop}$ first increases with μ for $\mu < 0.8$, indicating that coil flattening facilitates ring hopping, and then decreases for $\mu > 0.8$, indicating that suppressed chain fluctuations reduce the ring mobility. These observations are consistent with the trend in the diffusion coefficient D. In conclusion, the non-monotonic dependence of D on μ stems from the coupling effects, as shown in Fig. 5(d). Stretching flattens the coil block, which promotes the diffusion of the ring. However, stretching suppresses the fluctuation of the coil block, which inhibits diffusion. Besides, We found that the maximum value of D occurs at $\mu = 0.8$ for $N_{ring} = 10$ and moves to $\mu = 0.5$ for $N_{ring} = 14$. The optimal μ^* value shifteds to lower values as the ring size increaseds. This indicates that the coil block can be considered flattened under weak stretching for larger rings, and the sup-

pression of chain fluctuations by stretching plays a dominant role after μ^*.

Effects of the Ring Size N_{ring}

Furthermore, we investigated the sliding dynamics of a ring threaded on a rod-coil copolymer with a rod-to-coil ratio $\alpha=1$ and a relative extension of the coil block $\mu=0.23$. The mean-squared displacement $g_3(t)$ of the ring was measured for different ring size N_{ring}. As illustrated in Fig. 6, the $g_3(t)$ curves exhibit three distinct dynamical regimes, which is consistent with the behaviors observed in Figs. 2 and 4. In the short-time regime, the $g_3(t)$ curves closely overlap, $g_3(t) \sim t^{\beta}$ and $\beta \approx 1$, reflecting the normal diffusive motion of the ring along the rod or coil blocks. At long times, the ring dynamics exhibit long-time normal diffusion, where $g_3(t)$ increases with N_{ring}. However, when the ring size exceeded a certain threshold, a decrease in $g_3(t)$ wais observed. In the intermediate time scale, sub-diffusive behavior occurs, which is attributed to the heterogeneous architecture of the rod-coil copolymer backbone. The ring is confined to the rod block, and it is difficult for the ring to slide across the rod-coil interface into an adjacent coil block, which corresponds to the intermediate subdiffusion regime.

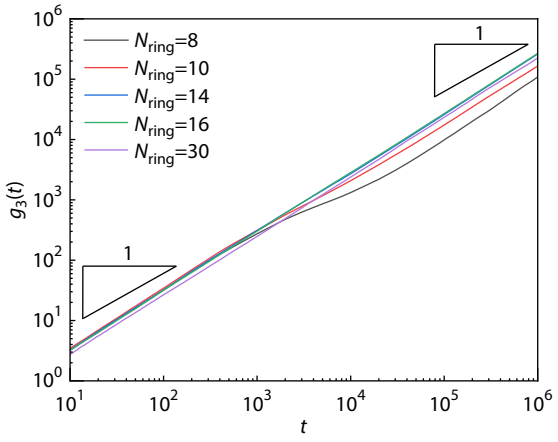

Fig. 6 Time dependence of $g_3(t)$ of the ring threaded on the rod-coil block polymer for different ring sizes N_{ring}. Here, the rod-coil length ratio is $\alpha = 1$ and the coil stretching degree is $\mu = 0.23$.

Finally, the dependence of the diffusion coefficient D on ring size, N_{ring} was examined. As shown in Fig. 7(a), the diffusion coefficient D of the rigid rings exhibits a nonmonotonic relationship with ring size N_{ring}. The radius of gyration, R_g, of the ring for different ring sizes, N_{ring} is calculated, and the results are shown in Fig. 7(b). Here $R_g = \sqrt{\langle R_g^2 \rangle}$. As shown in Fig. 7(b), R_g increaseds monotonically with N_{ring}. For $N_{ring} \le 16$, with an increase in N_{ring}, the friction between the ring and the rod-coil copolymer backbone gradually decreases, leading to an increase in D. However, for $N_{ring} \ge 20$, $R_g > 3$, where the ring sizes are sufficiently larger than the chain diameter. Hence, the interaction between the ring and backbone becomes negligible, and the sliding dynamics of the ring are mainly dominated by the diffusion of the ring. Because the diffusion coefficient is inversely proportional to the effective mass ($D_0 = \frac{k_B T}{\gamma M}$),[27] the diffusion coefficient of ring D decreases as N_{ring} increases. These results are consistent with those of a previous work.[27]

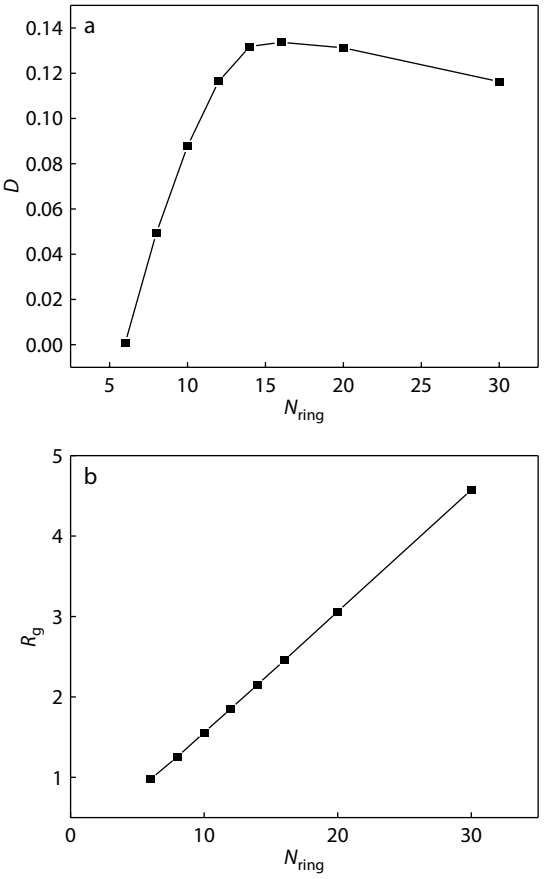

Fig. 7 (a) Diffusion coefficient D versus ring size N_{ring} for α=1 and μ=0.23; (b) Root-mean-square radius of gyration, R_g, of the ring for different ring sizes N_{ring}.

CONCLUSIONS

Based on the Kremer-Grest model, large-scale coarse-grained molecular dynamics simulations were performed to systematically investigate the sliding dynamics of rings along a rod-coil backbone in rotaxanes. The simulation results demonstrated that the sliding dynamics of the rings, characterized by the mean square displacement $g_3(t)$ and diffusion coefficient D, are systematically modulated by three key parameters: the rod-to-coil length ratio α, stretching degree of the coil block μ, and ring size N_{ring}. A key feature of the ring dynamics is the intermediate-time sub-diffusion in $g_3(t)$, which originates from the heterogeneity of the rod-coil copolymer. When the ring encounters the rod-coil interface, the ring's probability of crossing vanishes, marking the onset of the subdiffusive regime. After shuttling through Brownian motion, the ring slides through the interface and ends in this regime. First, the dependence of D on α exhibits a nonmonotonic variation, characterized by an initial decrease followed by an increase. This indicates that the more homogeneous the axial polymer chain is, the faster the ring diffuses. Then, the diffusion coefficient of ring D increases first and then decreases as μ increases, which suggests that the sliding

dynamics of the ring are governed by the competition between chain flattening and coil block fluctuation. In addition, ring size N_{ring} also has a non-monotonic influence on diffusion. D first increases and then decreases with increasing N_{ring}, which indicates that the sliding dynamics are dominated not only by the friction between the ring and the axial chain but also by the self-diffusion of the ring. This study provides molecular-level insights into how these dominant factors govern the sliding dynamics of rings in rod-coil-based rotaxanes and helps us to control the sliding dynamics in molecular designs.

Conflict of Interests

The authors declare no interest conflict.

Data Availability Statement

The related data are available from the authors upon reasonable request.

ACKNOWLEDGMENTS

This study was financially supported by the National Natural Science Foundation of China (Nos. 22403062, 22273067, and 12374215).

REFERENCES

1 Harrison, I.T.; Harrison, S. Synthesis of a stable complex of a macrocycle and a threaded chain. *J. Am. Chem. Soc.* **1967**, *89*, 5723–5724.
2 Gibson, H. W.; Bheda, M. C.; Engen, P. T. Rotaxanes, catenanes, polyrotaxanes, polycatenanes and related materials. *Prog. Polym. Sci.* **1994**, *19*, 843–945.
3 Harada, A.; Hashidzume, A.; Yamaguchi, H.; Takashima, Y. Polymeric rotaxanes. *Chem. Rev.* **2009**, *109*, 5974–6023.
4 Fang, L.; Olson, M. A.; Benítez, D.; Tkatchouk, E.; Goddard III, W. A.; Stoddart, J. F. Mechanically bonded macromolecules. *Chem. Soc. Rev.* **2010**, *39*, 17–29.
5 Winn, J.; Pinczewska, A.; Goldup, S.M. Synthesis of a rotaxane cui triazolide under aqueous conditions. *J. Am. Chem. Soc.* **2013**, *135*, 13318–13321.
6 Leigh, D. A.; Marcos, V.; Wilson, M. R., Rotaxane catalysts. *ACS Catal.*, **2014**, *4*, 4490–4497.
7 Sauvage, J. P. From chemical topology to molecular machines (nobel lecture). *Angew. Chem. Int. Ed.* **2017**, *56*, 11080–11093.
8 Mena-Hernando, S.; Pérez, E. M. Mechanically interlocked materials. Rotaxanes and catenanes beyond the small molecule. *Chem. Soc. Rev.* **2019**, *48*, 5016–5032.
9 Takata, T. Polyrotaxane and polyrotaxane network: Supramolecular architectures based on the concept of dynamic covalent bond chemistry. *Polym. J.* **2006**, *38*, 1–20.
10 Harada, A.; Takashima, Y.; Yamaguchi, H. Cyclodextrin-based

Graphical Abstract

Sliding Dynamics of Ring Chain on a Rod-coil Block Copolymer in Rotaxane

Si-Yi Yan, Xiang-Hong Wang, Ke Li, and Lin-Li He

Wenzhou University; Shanghai Technical Institute of Electronics & Information; Shanghai University of Electric Power

The sliding dynamics of the ring chain in rod-coil rotaxanes depend non-monotonically on the rod-coil ratio a, coil stretch μ, and ring size. Intermediate-time sub-diffusion arises from backbone heterogeneity. Diffusion is fastest on homogeneous chains and under moderate coil stretching, thereby guiding the design of tunable slide-ring materials.

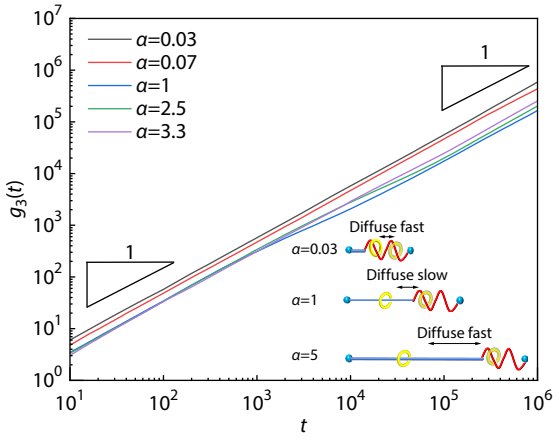

Chinese J. Polym. Sci., 2026 *https://doi.org/10.1007/s10118-026-3711-9*

supramolecular polymers. *Chem. Soc. Rev.* **2009**, *38*, 875–882.
11 Loethen, S.; Ooya, T.; Choi, H. S.; Yui, N.; Thompson, D. H. Synthesis, characterization, and ph-triggered dethreading of α-cyclodextrin-poly(ethylene glycol) polyrotaxanes bearing cleavable endcaps. *Biomacromolecules* **2006**, *7*, 2501–2506.
12 Araki, J.; Kataoka, T.; Ito, K. Preparation of a "sliding graft copolymer", an organic solvent-soluble polyrotaxane containing mobile side chains, and its application for a crosslinked elastomeric supramolecular film. *Soft Matter* **2008**, *4*, 245–249.
13 Harada, A.; Li, J.; Kamachi, M. The molecular necklace: A rotaxane containing many threaded α-cyclodextrins. *Nature* **1992**, *356*, 325–327.
14 Okumura, Y.; Ito, K. The polyrotaxane gel: a topological gel by figure-of-eight cross-links. *Adv. Mater.* **2001**, *13*, 485–487.
15 Zhu, K.; Baggi, G.; Loeb, S. J. Ring-through-ring molecular shuttling in a saturated [3] rotaxane. *Nat. Chem.* **2018**, *10*, 625–630.
16 Bruns, C. J.; Stoddart, J. F. Rotaxane-based molecular muscles. *Acc. Chem. Res.* **2014**, *47*, 2186–2199.
17 Juluri, B. K.; Kumar, A. S.; Liu, Y.; Ye, T.; Yang, Y. W.; Flood, A. H.; Fang, L.; Stoddart, J. F.; Weiss, P. S.; Huang, T. J. A mechanical actuator driven electrochemically by artificial molecular muscles. *Acs Nano* **2009**, *3*, 291–300.
18 Iwaso, K.; Takashima, Y.; Harada, A. Fast response dry-type artificial molecular muscles with [c2] daisy chains. *Nat. Chem.* **2016**, *8*, 625–632.
19 Anelli, P. L.; Spencer, N.; Stoddart, J. F. A molecular shuttle. *J. Am. Chem. Soc.* **1991**, *113*, 5131–5133.
20 Clavel, C.; Romuald, C.; Brabet, E.; Coutrot, F. A ph-sensitive lasso-based rotaxane molecular switch. *Chem. Eur. J.* **2013**, *19*, 2982–2989.
21 Murakami, H.; Kawabuchi, A.; Kotoo, K.; Kunitake, M.; Nakashima, N. A light-driven molecular shuttle based on a rotaxane. *J. Am. Chem. Soc.* **1997**, *119*, 7605–7606.
22 Müller, T.; Sommer, J.; Lang, M. Tendomers - force sensitive bis-rotaxanes with jump-like deformation behavior. *Soft Matter* **2019**, *15*, 3671–3679.
23 Müller, T.; Sommer, J.; Lang, M. Swelling of tendomer gels. *Macromolecules* **2021**, *54*, 4601–4614.
24 Mills, P.; Mayer, J.; Kramer, E.; Hadziioannou, G.; Lutz, P.; Strazielle, C.; Rempp, P.;Kovacs, A. Diffusion of polymer rings in linear polymer matrices. *Macromolecules* **1987**, *20*, 513–518.
25 Metzler, R.; Kantor, Y.; Kardar, M. Force-extension relations for polymers with sliding links. *Phys. Rev. E* **2002**, *66*, 022102.
26 Brackley, C.; Johnson, J.; Michieletto, D.; Morozov, A.; Nicodemi, M.; Cook, P.;Marenduzzo, D. Nonequilibrium chromosome looping *via* molecular slip links. *Phys. Rev. Lett.* **2017**, *119*, 138101–138101.
27 Yasuda, Y.; Toda, M.; Mayumi, K.; Yokoyama, H.; Morita, H.;Ito, K. Sliding dynamics of ring on polymer in rotaxane: a coarse-grained molecular dynamics simulation study. *Macromolecules* **2019**, *52*, 3787–3793.
28 Mayumi, K. Molecular dynamics and structure of polyrotaxane in solution. *Polym. J.* **2021**, *53*, 581–586.
29 Uenuma, S.; Maeda, R.; Takahashi, S.; Kato, K.; Yokoyama, H.; Ito, K. Self-assembled structure of polyrotaxane consisting of *β*-cyclodextrin and poly(ethylene oxide)-block-poly(propylene oxide)-block-poly(ethylene oxide) triblock copolymer in bulk system. *Chem. Lett.* **2016**, *45*, 991–993.
30 Wu, H.; He, L.; Wang, X.; Wang, Y.; Jiang, Z. Liquid crystalline assembly of rod-coil diblock copolymer and homopolymer blends by dissipative particle dynamics simulation. *Soft Matter* **2014**, *10*, 6278–6285.
31 Lin, Y. L.; Chang, H. Y.; Sheng, Y. J.; Tsao, H. K. Structural and mechanical properties of polymersomes formed by rod-coil diblock copolymers. *Soft Matter* **2013**, *9*, 4802–4814.
32 Olsen, B.; Segalman, R. Self-assembly of rod-coil block copolymers. *Mater. Sci. Eng. R Rep.* **2008**, *62*, 37–66.
33 Gao, L.; Lin, J.; Zhang, L.; Wang, L. Living supramolecular polymerization of rod-coil block copolymers: Kinetics, origin of uniformity, and its implication. *Nano Lett.* **2019**, *19*, 2032–2036.
34 Wang, Y.; Lu, H.; Jia, X.; Shi, A.; Zhou, J.; Zhang, G.; Liu, H. Entropy-induced localization and sliding dynamics of rings on polyrotaxane. *Macromolecules* **2024**, *57*, 1846–1858.
35 Uenuma, S.; Maeda, R.; Kato, K.; Mayumi, K.; Yokoyama, H.; Ito, K. Drastic change of mechanical properties of polyrotaxane bulk: Aba-bab sequence change depending on ring position. *Acs Macro Lett.* **2019**, *8*, 140–144.
36 Niu, Y.; Wang, Y.; Su, W.; Liu, Z.; Yang, D.H.; Wang, J.; Feng, Z.;Ye, L. Polymer modified cyclodextrin-based polyrotaxanes: From functionalization to applications. *Prog. Mater. Sci.* **2026**, *160*, 101676.
37 Wang, Y.; Niu, Y.; Geng, X.; Feng, Z.; Ye, L. The motility of *β*-cyclodextrins threaded on the polyrotaxane based triblock polymer and its influences on mechanical properties. *Materials* **2024**, *17*, 1996–1944.
38 Liu, S.; Watanabe, K.; Miwa, E.; Hara, M.; Seki, T.; Mayumi, K.; Ito, K.; Takeoka, Y. Mechanical properties of polymer networks with polyrotaxane crosslinkers with different molecular structures based on polyethylene glycol and α-cyclodextrin. *Giant* **2024**, *17*, 100224.
39 Mayumi, K.; Liu, C.; Yasuda, Y.; Ito, K. Softness, elasticity, and toughness of polymer networks with slide-ring cross-links. *Gels* **2021**, *7*, 91.
40 Zhu, S. S.; Carroll, P. J.; Swager, T. M. Conducting polymetallorotaxanes: a supramolecular approach to transition metal ion sensors. *J. Am. Chem. Soc.* **1996**, *118*, 8713–8714.
41 Zhu, S.; Swager, T. Conducting polymetallorotaxanes: Metal ion mediated enhancements in conductivity and charge localization. *J. Am. Chem. Soc.* **1997**, *119*, 12568–12577.
42 Jäger, R.; Händel, M.; Harren, J.; Vögtle, F.; Rissanen, K. Chemistry with roataxanes: Intra-and intermolecularly covalently linked rotaxanes. *Liebigs Ann.* **1996**, *1996*, 1201–1207.
43 Rapaport, D. C., in *The art of molecular dynamics simulation*. Cambridge university press, Cambridge, **1995**.
44 Frenkel, D.; Smit, B., in *Understanding molecular simulation: From algorithms to applications*. Academic Press, San Diego, CA, **1996**.
45 Kremer, K.; Grest, G.S. Dynamics of entangled linear polymer melts: a molecular-dynamics simulation. *J. Chem. Phys.* **1990**, *92*, 5057–5086.
46 Weeks, J.D.; Chandler, D.; Andersen, H.C. Role of repulsive forces in determining the equilibrium structure of simple liquids. *J. Chem. Phys.* **1971**, *54*, 5237–5247.
47 Gilles, F.; Llubaroff, R.; Pastorino, C. Fluctuation-induced forces between rings threaded around a polymer chain under tension. *Phys. Rev. E* **2016**, *94*, 032503.
48 Luo, K.; Ala-Nissila, T.; Ying, S.; Bhattacharya, A. Sequence dependence of DNA translocation through a nanopore. *Phys. Rev. Lett.* **2008**, *100*, 058101.
49 Pei, H. W.; Liu, H.; Lu, Z. Y.; Zhu, Y. L. Tuning surface wettability by designing hairy structures. *Phys. Rev. E* **2015**, *91*, 020401.
50 Guo, F.; Li, K.; Wu, J.; Wang, Y.; Zhang, L. Sliding dynamics of ring chain on a knotted polymer in rotaxane. *Polymer* **2021**, *235*, 124226.
51 Turq, P.; Lantelme, F.; Friedman, H.L. Brownian dynamics: Its application to ionic solutions. *J. Chem. Phys.* **1977**, *66*, 3039–3044.
52 Grest, G.S.; Kremer, K. Molecular dynamics simulation for polymers in the presence of a heat bath. *Phys. Rev. A* **1986**, *33*, 3628.
53 Plimpton, S. Fast parallel algorithms for short-range molecular dynamics. *J. Comput. Phys.* **1995**, *117*, 1–19.
54 Yasuda, Y.; Hidaka, Y.; Mayumi, K.; Yamada, T.; Fujimoto, K.; Okazaki, S.; Yokoyama, H.; Ito, K. Molecular dynamics of polyrotaxane in solution investigated by quasi-elastic neutron scattering and molecular dynamics simulation: sliding motion of rings on polymer. *J. Am. Chem. Soc.* **2019**, *141*, 9655–9663.
55 Bedrov, D.; Smith, G.D.; Smith, J.S. Matrix-induced nanoparticle interactions in a polymer melt: A molecular dynamics simulation study. *J. Chem. Phys.* **2003**, *119*, 10438–10447.